NATIONAL ADVISORY COMMITTEE FOR AERONAUTICS

TECHNICAL NOTE 2184

INVESTIGATION OF FREQUENCY-RESPONSE CHARACTERISTICS OF ENGINE SPEED FOR A TYPICAL TURBINE-PROPELLER ENGINE

By Burt L. Taylor, III, and Frank L. Oppenheimer

Lewis Flight Propulsion Laboratory
Cleveland, Ohio

Washington
September 1950

NATIONAL ADVISORY COMMITTEE FOR AERONAUTICS

TECHNICAL NOTE 2184

INVESTIGATION OF FREQUENCY-RESPONSE CHARACTERISTICS OF ENGINE SPEED FOR A TYPICAL TURBINE-PROPELLER ENGINE

By Burt L. Taylor, III, and Frank L. Oppenheimer

SUMMARY

Experimental frequency-response characteristics of engine speed for a typical turbine-propeller engine are presented. These data were obtained by subjecting the engine to sinusoidal variations of fuel flow and propeller-blade-angle inputs. Correlation is made between these experimental data and analytical frequency-response characteristics obtained from a linear differential equation derived from steady-state torque-speed relations.

The results of this investigation indicate that engine speed is a linear function of fuel flow and propeller-blade angle for limited variations of these parameters. Algebraic expressions approximately describing the frequency-response characteristics of the engine tested are primarily first order. Approximate frequency-response characteristics limited to first-order effects may be calculated from solutions of a linear differential equation and equilibrium torque characteristics of the engine and the propeller.

INTRODUCTION

In order to design controls that will provide desirable transient operation, the dynamics of the various components of the controlled system should be known. The most general description of the dynamics of any system is the differential equations of motion, but use of the detailed and precise aerodynamic and thermodynamic equations for analysis of dynamic behavior of a gas-turbine engine and control system presents insurmountable problems. On the other hand, any description whereby linear behavior of the system components is assumed can be placed in a form that is readily handled and productive of results. The advantages of the linear assumption are so far-reaching that its use is justified, even

where the system is of known nonlinearity but where high precision of results is not required, such as in the investigation of controls for gas-turbine engines.

In the linear field, several descriptive forms can be used. The most general of these is the frequency response, whereby the attenuation and the phase lag of steady sinusoidal inputs are given for the continuous frequency spectrum. When these data are available for each component of a closed-loop control system, the time response of the system can be calculated. By employing techniques of analysis and synthesis described in reference 1, system behavior can be altered to obtain desired frequency-response characteristics and the related time response.

A general investigation is in progress at the NACA Lewis laboratory to determine the nature of the dynamics of gas-turbine power plants and to devise and to evaluate methods for describing this behavior in a form applicable to control synthesis and analysis. Special emphasis has been placed on the determination of the behavior of rotative speed because of its importance in this type of engine for safety and optimum operation. The results of an investigation of the frequency-response characteristics of a turbine-propeller engine are presented herein. Experimental frequency-response data were analyzed to obtain the general form and nature of the frequency-response and dynamic characteristics of such engines, to verify the linear assumption, and to obtain a basis upon which other descriptive forms of the dynamic behavior may be compared. One such comparison is made between the linear differential equation obtained from equilibrium-torque curves and experimental frequency-response characteristics.

For purposes of this investigation, the dynamic response of engine speed to disturbances in fuel flow and propeller-blade angle for a typical turbine-propeller engine is used.

ANALYSIS

Development of Linear Differential Equations

With the hypothesis that quasi-static conditions exist in an engine during transient conditions of operation, a differential equation may be derived to express the behavior of engine speed as a function of fuel flow (reference 2). An assumption is made that the torque output of the engine is some function of only two variables, engine speed and fuel flow, for a given condition of

altitude and ram pressure ratio. This function may be expanded and linearized so that the following equation approximates the behavior of engine speed for operation in a small region

$$\left.\begin{aligned} Q_e &= f_1(W_f, N_e) \\ \Delta Q_e &= a\Delta W_f - b\Delta N_e \end{aligned}\right\} \tag{1}$$

where a is the partial derivative of engine torque with respect to fuel flow and b is the absolute value of the partial derivative of engine torque with respect to engine speed. A delta prefix before a variable signifies deviation from the initial operating point. (All symbols used in this report are defined in the appendix.)

In a similar manner, the torque absorbed by a propeller may be expressed as some function of rotational speed and blade angle

$$\left.\begin{aligned} Q_p &= f_2(\beta, N_p) \\ \Delta Q_p &= c\Delta\beta + d\Delta N_p \\ \Delta Q_p &= c\Delta\beta + \frac{d}{R}\Delta N_e \end{aligned}\right\} \tag{2}$$

where c is the partial derivative of propeller torque with respect to blade angle and where d is the partial derivative of propeller torque with respect to propeller speed.

Any unbalance between torque developed by the engine and torque absorbed by the propeller results in an acceleration. If the effective moment of inertia is assumed to be comprised of the propeller and the rotating parts of the engine, the unbalanced torque may be expressed in terms of engine speed and the moments of inertia by the following equation:

$$\Delta Q_e - \frac{\Delta Q_p}{R} = \left(I_e + \frac{I_p}{R^2}\right)\dot{\Delta N}_e \tag{3}$$

If equation (2) is divided by the gear ratio R and subtracted from equation (1), the following equation results:

$$\Delta Q_e - \frac{\Delta Q_p}{R} = a\Delta W_f - \frac{c}{R}\Delta\beta - \left(b + \frac{d}{R^2}\right)\Delta N_e \tag{4}$$

Equations (3) and (4) may be combined, yielding the following differential equation relating engine speed to fuel flow and blade angle:

$$\left(I_e + \frac{I_p}{R^2}\right)\dot{\Delta N}_e + \left(b + \frac{d}{R^2}\right)\Delta N_e = a\Delta W_f - \frac{c}{R}\Delta\beta \qquad (5)$$

If equation (5) is divided through by $N_{e(max)}$ and $\left(I_e + \frac{I_p}{R^2}\right)$ and the appropriate terms divided by $\frac{N_{e(max)}}{N_{e(max)}}$, $\frac{N_{p(max)}}{N_{p(max)}}$, or $\frac{W_{f(max)}}{W_{f(max)}}$, the following dimensionless equation expressing speed and fuel flow is obtained:

$$\left(\frac{I_e+\frac{I_p}{R^2}}{I_e+\frac{I_p}{R^2}}\right)\frac{\Delta\dot{N}_e}{N_{e(max)}}+\left\{\left[\frac{\partial Q_e}{\frac{\partial N_e}{N_{e(max)}}}\right]\left[\frac{1}{N_{e(max)}}\right]\left(\frac{1}{I_e+\frac{I_p}{R^2}}\right)+\left[\frac{\partial Q_p}{\frac{\partial N_p}{N_{p(max)}}}\right]\left(\frac{1}{R^2}\right)\left[\frac{1}{N_{p(max)}}\right]\left(\frac{1}{I_e+\frac{I_p}{R^2}}\right)\right\}\frac{\Delta N_e}{N_{e(max)}}$$

$$=\left[\frac{\partial Q_e}{\frac{\partial W_f}{W_{f(max)}}}\right]\left[\frac{1}{W_{f(max)}}\right]\left[\frac{1}{N_{e(max)}}\right]\left(\frac{1}{I_e+\frac{I_p}{R^2}}\right)\Delta W_f-\left(\frac{\partial Q_p}{\partial\beta}\right)\left(\frac{1}{R}\right)\left[\frac{1}{N_{e(max)}}\right]\left(\frac{1}{I_e+\frac{I_p}{R^2}}\right)\Delta\beta$$

$$\frac{\Delta\dot{N}_e}{N_{e(max)}}+\left\{\frac{\partial\left[\frac{Q_e}{N_{e(max)}\ I_e\left(1+\frac{I_p/R^2}{I_e}\right)}\right]}{\partial\left[\frac{N_e}{N_{e(max)}}\right]}+\frac{\partial\left[\frac{Q_p}{N_{p(max)}\ I_p\left(1+\frac{I_e}{I_p/R^2}\right)}\right]}{\partial\left[\frac{N_p}{N_{p(max)}}\right]}\right\}\frac{\Delta N_e}{N_{e(max)}}$$

$$=\frac{\partial\left[\frac{Q_e}{N_{e(max)}\ I_e\left(1+\frac{I_p/R^2}{I_e}\right)}\right]}{\partial\left[\frac{W_f}{W_{f(max)}}\right]}\frac{\Delta W_f}{W_{f(max)}}-\frac{\partial\left[\frac{Q_p}{N_{p(max)}\ I_p\left(1+\frac{I_e}{I_p/R^2}\right)}\right]}{\partial[\beta]}\Delta\beta$$

$$\frac{\Delta\dot{N}_e}{N_{e(max)}}+(b_1+d_1)\frac{\Delta N_e}{N_{e(max)}}=a_1\frac{\Delta W_f}{W_{f(max)}}-c_1\Delta\beta \qquad (6)$$

The form of equation (6) is that of a first-order lag, which can be written as follows:

$$\tau \frac{\Delta \dot{N}_e}{N_{e(max)}} + \frac{\Delta N_e}{N_{e(max)}} = K_1 \frac{\Delta W_f}{W_{f(max)}} - K_2 \Delta\beta \tag{7}$$

where the dynamic characteristics are entirely defined by the time constant τ and the equilibrium condition is defined by K_1 and K_2. Thus,

$$\left.\begin{aligned} \tau &= \frac{1}{b_1 + d_1} \\ K_1 &= \frac{a_1}{b_1 + d_1} \\ K_2 &= \frac{c_1}{b_1 + d_1} \end{aligned}\right\} \tag{8}$$

Frequency Response

Frequency-response characteristics may be calculated by solving the differential equation describing a system subjected to sinusoidal forcing functions of various frequencies. The same results may be obtained by applying the operational calculus to the differential equation. Thus, the response of engine speed to fuel flow at constant blade angle can be expressed in terms of the operator $i\omega$ as follows:

$$\frac{\dfrac{\Delta N_e}{N_{e(max)}}}{\dfrac{\Delta W_f}{W_{f(max)}}}(i\omega) = \frac{K_1}{(1 + i\tau\omega)} \tag{9}$$

which is obtained from equation (7) by replacing the first derivative with respect to time by $(i\omega)$ and treating the results algebraically. The complex operator represents both the ratio of the amplitudes of the engine-speed and fuel-flow sine waves and the relative phase angles. The amplitude ratio is the absolute value of the complex function, as follows:

$$\left| \frac{\frac{\Delta N_e}{N_{e(max)}}}{\frac{\Delta W_f}{W_{f(max)}}} \right| = \frac{K_1}{\sqrt{1 + \tau^2\omega^2}} \tag{10}$$

The angle by which the engine-speed sine wave lags the fuel-flow sine wave is as follows:

$$\text{Ang} \frac{\frac{\Delta N_e}{N_{e(max)}}}{\frac{\Delta W_f}{W_{f(max)}}} = \tan^{-1}(\omega\tau) \tag{11}$$

The frequency response of engine speed to blade angle at constant fuel flow may be obtained by the same procedure,

$$\frac{\frac{\Delta N_e}{N_{e(max)}}}{\Delta\beta}(i\omega) = \frac{K_2}{(1 + i\tau\omega)} \tag{12}$$

$$\left| \frac{\frac{\Delta N_e}{N_{e(max)}}}{\Delta\beta} \right| = \frac{K_2}{\sqrt{1 + \tau^2\omega^2}} \tag{13}$$

$$\text{Ang} \frac{\frac{\Delta N_e}{N_{e(max)}}}{\Delta\beta} = \tan^{-1}(\omega\tau) \tag{14}$$

APPARATUS AND PROCEDURE

Engine Installation

Engine. - The principal components of the engine used for the investigation are an axial-flow compressor, reverse-flow combustion chambers, and a single-stage direct-coupled turbine. A two-stage planetary gear system provides a speed reduction between the turbine and the propeller.

A 12-foot-1-inch-diameter, four-bladed propeller was installed on the engine. The pitch-changing mechanism is a self-contained hydraulic unit located in the propeller hub. A lever, or beta arm, on the stationary portion of the hub operates the hydraulic control valves in the rotating part so that a linear relation exists between the beta arm and the blade angle. Each position of the beta arm corresponds to a unique blade angle during steady-state operation.

Harmonic-motion generator. - An approximation of simple harmonic motion by the beta arm was obtained by connecting it to a rotating crank driven by a direct-current motor through a worm-gear reduction unit. A minimum ratio of 100:1 between the connecting rod and the crank length made the motion of the beta arm vary less than 1 percent from a true sine wave. By controlling the armature current and substituting various speed reducers in the harmonic-motion generator, a range of frequencies could be obtained. The center of amplitude of the sine wave could be varied by shifting the position of the harmonic-motion generator, and various amplitudes could be obtained by changing the crank length.

In order to vary fuel flow sinusoidally, the fuel system of the engine was disconnected from the manifold and replaced by an external system, as shown in figure 1. A line was connected in parallel with the main throttle in order to obtain a small variation of fuel input about a center of amplitude set by the main throttle. The harmonic-motion generator used in the blade-angle runs was used to vary the flow in the parallel line by means of a linear valve. Changes in pressure drop across the valve were too small to have an effect upon the linear variation of flow during transient operation.

Instrumentation

Steady-state measurements were taken of propeller-blade angle, fuel flow, engine torque, and engine speed. Provisions were made to measure all of these variables except the torque during transient conditions of operation.

Blade-angle position was measured by the use of a potentiometer attached to the propeller blade that varied the flow of current in an electric circuit in direct proportion to the blade position. For steady-state measurements, the current was measured by a milliammeter; during transient conditions the circuit was switched to a recording oscillograph element. A conventional slip-ring

arrangement was used to complete the circuit between the potentiometer on the propeller hub and the recording device. Beta-arm position was recorded in a similar manner.

In order to measure fuel flow, an A.S.M.E. orifice was installed in the main fuel line immediately upstream of the engine fuel manifold. A bellows-type differential-pressure gage measured the pressure drop across the orifice and actuated a small potentiometer that varied the current in a circuit similar to that used for blade-angle measurement. Inasmuch as flow variations were small in comparison to mean flow, the nonlinear relation between pressure drop and actual flow was insignificant.

The ring gear of the planetary reduction unit of the engine is restrained by a self-balancing hydraulic system. The torque output of the engine was indicated by the pressure required to act on the hydraulic piston to maintain balance. This pressure was measured by a Bourdon gage.

Steady-state measurement of engine speed was accomplished by means of a three-phase tachometer generator and indicator. For recording transients in engine speed on the oscillograph, a direct-current tachometer generator was utilized in a current-measuring circuit.

A 10-cycle-per-second timing signal generated by an audio-oscillator was recorded on the oscillograph film to show the time variation of the measured variables. The signal was frequently compared to a standard 60-cycle-per-second current on a cathode-ray oscilloscope for calibration purposes.

Schematic diagrams of the transient measurement circuits are shown in figure 2. Table I indicates the steady-state and transient characteristics of the instruments used. The oscillograph was used to record only increments of deviation from the initial operating point. Conventional steady-state instruments were used to measure the level at which the transient occurred and to evaluate the increments. The oscillograph was calibrated frequently during the runs for known values of deviation as measured by the steady-state instruments.

Procedure

Frequency-response runs. - In order to determine the frequency response of engine speed, sinusoidal variations were made in

propeller-blade angle at constant fuel flow and in fuel flow at constant blade angle. The frequency range to be investigated was determined by the following considerations: It is shown in reference 1 that for a first-order system the break frequency is inversely proportional to the system time constant and that an adequate frequency range to describe the unit is 0.1 to 10 times this value. Therefore, by assuming the time constant to be 5 seconds and considering the engine primarily of first order, the range of descriptive frequencies was defined to be 0.02 to 2 radians per second.

Dynamic behavior about two equilibrium running conditions of the engine was investigated. The first condition was 65 percent of maximum rated fuel flow and a blade angle of 18° (97.5 percent of maximum engine speed). The other condition was 81 percent of maximum rated fuel flow and a blade angle of 28° (92.5 percent of maximum engine speed). The amplitude of the forcing function was the same at each operating condition; namely, a blade angle of 2° and 3.9 percent of maximum rated fuel flow. For each run, oscillographic records were made of the time variation of pertinent variables during steady-state sinusoidal operation. Typical records of these data are reproduced in figure 3. The high frequency variation of the fundamental waves in these figures resulted from electrical and mechanical disturbances to the sensing elements.

Equilibrium runs. - Equilibrium data required to evaluate the constants of equation (6) were obtained by the following procedure: For a set value of fuel flow, propeller-blade angle was adjusted to obtain nine operating points between 85 and 100 percent of maximum engine speed. These speed points were used for fuel flows of 50.0, 57.6, 65.4, 69.1, 77.0, and 84.5 percent of maximum fuel flow except when torque or turbine-outlet-temperature limitations prohibited operation throughout the complete range. Engine torque, engine speed, fuel flow, and blade-angle measurements were taken at each operating point.

RESULTS AND DISCUSSION

Experimentally Determined Frequency-Response Characteristics

Results of sinusoidal inputs. - Results of the sinusoidal blade-angle and fuel-flow inputs as obtained from the oscillographic traces are shown in figures 4 and 5. Amplitude ratio of output to

input is presented on log-log coordinates as a function of frequency. Phase-angle lag of the output relative to input is presented on semilog coordinates as a function of frequency.

The form of these frequency-response curves indicates the nature of the dynamic characteristics of this power plant. The regularity of data points indicates that the system follows these predicted characteristics better than might be anticipated. Furthermore, in support of the assumptions made for the differential-equation analysis, the system appears to be primarily a first-order lag system. Despite the complexity of the physical system and the processes performed in the turbine cycle, a fairly simple mathematical form approximates the actual behavior of the engine.

Algebraic form of data. - As shown in figures 4 and 5, although the system is primarily first order, higher order effects are present. Increased attenuation of the output amplitude at phase shifts approaching 180° indicates that a second-order approximation may more exactly describe the data. An equation of the following form has therefore been fitted to the experimental data:

$$\frac{\text{output}}{\text{input}} = \frac{K}{(1 + i\tau_1\omega)(1 + i\tau_2\omega)}$$

The equation was matched to the experimental data at the steady-state point and at phase shifts of 45° and 90°, thereby determining the three variables of the equation, K, τ_1, and τ_2. Results of these computations are presented in column 3 of table II.

A maximum error in the value of the second time constant τ_2 of 0.1 second could be attributed to instrument lags; the numerical values for this time constant τ_2 are therefore presented only to indicate the order of magnitude of this second-order effect. Because the fuel-measurement device was slower than the blade-angle measurement circuit, instrumentation error would reduce the value of τ_2 in the functions of engine speed to fuel flow input. The opposite trend of experimental results indicates that the second-order effect is an engine phenomenon. The fact that a ratio in the order of 10:1 exists between the two time constants τ_1 and τ_2 makes the second-order effect negligible for many problems of control analysis.

In order to compare the form of the algebraic approximations with the actual data, cross plots of figures 4 and 5 are presented on figures 6 and 7, respectively, together with curves of the algebraic expressions. The calculated first-order curves of figures 6 and 7 will be subsequently discussed.

Comparison of frequency-response functions. - Variation of the first-order time constant with operating conditions may be of more importance than the second-order effect. A comparison of first-order time constants in table II shows that these constants not only vary with the engine-power points but also vary with the forcing function at the same power point. For an exact description of dynamic behavior of engine speed, extensive data may be required to determine the trend of transient characteristics.

Linearity of dynamic behavior. - For purposes of analysis, an assumption was made that engine speed was a linear function of fuel flow and blade angle for small transients. In order to evaluate this assumption from the results of experimental data, the form of the outputs recorded on oscillographic film were compared to an analytical sine wave. It was found that for inputs resulting in engine-speed changes of as much as 6 percent of maximum speed the form of the speed sine wave varied negligibly from an exact sine wave. Greater input amplitudes resulting in larger speed oscillations caused appreciable distortion, the effect being greater at low-power points. An assumption of linearity is therefore justified only for restricted deviations on the order of 3 or 4 percent from an equilibrium point.

Analytically Determined Frequency-Response Characteristics

Results of equilibrium runs. - The relation between steady-state values of engine torque and fuel flow is plotted in figure 8(a) for several values of constant speed. Cross plots for lines of constant fuel flow are shown in figure 8(b). Figure 9(a) is a plot of propeller torque against blade angle for various values of constant speed and cross plots for lines of constant blade angle are shown in figure 9(b). In order to show the equilibrium running conditions about which sinusoidal data were taken, two lines of constant blade angle, 18° and 28°, are superimposed on figure 8(b).

Losses to the accessories and the gear-reduction unit were neglected in calculations of propeller torque.

Range of linearity. - In the derivation of equations (1) and (2), an assumption was made that the relations presented in figures 8 and 9 may be considered as straight lines for small deviations from a given steady-state point. The actual data indicate that this assumption is justified for the engine characteristics over rather large regions, but the propeller characteristics should

be considered linear only in very small regions. Furthermore, these engine data as obtained under steady-state conditions of operation may not be accurate under transient conditions if the turbine is required to operate at a point far from the design condition (reference 2).

Analytical sinusoidal response. - Frequency-response characteristics of the engine were calculated for operating points at which experimental sinusoidal data were taken. Values of the constants a_1, b_1, c_1, and d_1 for an operating condition were obtained from the slopes of the curves of figures 8(a), 8(b), 9(a), and 9(b), respectively. With values so determined, equations (10), (11), (13), and (14) were evaluated for a range of frequencies coinciding with that used in the experimental runs. Results of these calculations are included in figures 6 and 7.

Algebraic form of analytical results. - The algebraic form of the first-order curves presented in figures 6 and 7 is shown in equations (9) and (12). These equations were evaluated for the selected operating points and the results are presented in column 4 of table II.

For the assumptions made in the analysis, the engine time constant is independent of the forcing function, as shown in equation (7). Variation of time constants for the two power points results from the nonlinearity of torque-speed characteristics of the engine and the propeller. The magnitude of this variation is sufficient to limit the utility of an analysis in which linear approximations are assumed. For studies of behavior within restricted regions, the analysis is satisfactory.

Comparison of Differential-Equation Solution with Experimental Results

Comparison of form. - Calculated frequency-response characteristics are similar to the experimental results at low-frequency values, as shown by figures 6 and 7. Because of higher-order effects exhibited by the experimental data, deviation between the two sets of curves increases at higher frequencies. This effect is particularly evident in the phase shift occurring at high frequencies. Presence of phase shifts greater than 90° in the engine system may limit the over-all loop gain for stability in a combined engine and control system. For the usual case in which the control contributes at least 90° additional phase shift to the engine polar diagram, the gain at the 180° phase shift point has a definite limit according to the Nyquist criterion (reference 1).

Comparison of numerical values. - In general, the value of the experimental time constant is lower than the value of the analytical time constant for a given power operating point. The significance of this variation depends on the particular application of the data; for some problems of control analysis a range of variation of 2 to 1 in the engine time constant causes little change in the combined engine-control system. Discrepancies between steady-state gain values, analytical and experimental, can be accounted for by the fact that the analytical values are calculated from slopes of equilibrium-torque curves.

CONCLUSIONS

From a sea-level static investigation of the frequency-response characteristics of a turbine-propeller engine, the following conclusions may be drawn:

1. Engine speed is a linear function of fuel flow and propeller-blade angle during transient operation, if deviations from the equilibrium operating point are on the order of 3 or 4 percent.

2. The frequency-response functions of engine speed to fuel flow and engine speed to blade angle are primarily first order, but higher-order effects exist.

3. A differential equation that closely describes engine speed as a function of fuel flow and blade angle can be derived from steady-state data.

Lewis Flight Propulsion Laboratory,
National Advisory Committee for Aeronautics,
Cleveland, Ohio, March 24, 1950.

APPENDIX - SYMBOLS

The following symbols are used throughout this report:

a partial derivative of engine torque with respect to fuel flow, $\left(\frac{\partial Q_e}{\partial W_f}\right)$, $\frac{\text{lb-ft}}{\text{lb/hr}}$

a_1 partial derivative of engine-torque parameter with respect to percentage maximum fuel flow, $\frac{\partial \frac{Q_e}{N_{e(max)}\, I_e \left[1 + \frac{I_p/R^2}{I_e}\right]}}{\partial \frac{W_f}{W_{f(max)}}}$, $\frac{1}{\text{sec}}$

b absolute value of partial derivative of engine torque with respect to engine speed, $\left(\frac{\partial Q_e}{\partial N_e}\right)$, $\frac{\text{lb-ft}}{\text{rpm}}$

b_1 partial derivative of engine-torque parameter with respect to percentage maximum engine speed, $\frac{\partial \frac{Q_e}{N_{e(max)}\, I_e \left[1 + \frac{I_p/R^2}{I_e}\right]}}{\partial \frac{N_e}{N_{e(max)}}}$, $\frac{1}{\text{sec}}$

c partial derivative of propeller torque with respect to blade angle, $\left(\frac{\partial Q_p}{\partial \beta}\right)$, $\frac{\text{lb-ft}}{\text{deg}}$

c_1 partial derivative of propeller-torque parameter with respect to blade angle, $\frac{\partial \frac{Q_p}{N_{p(max)}\, I_p \left[1 + \frac{I_e}{I_p/R^2}\right]}}{\partial \beta}$, $\frac{1}{(\text{sec})(\text{deg})}$

d partial derivative of propeller torque with respect to propeller speed, $\left(\frac{\partial Q_p}{\partial N_p}\right)$, $\frac{\text{lb-ft}}{\text{rpm}}$

d_1 partial derivative of propeller-torque parameter with respect to percentage maximum propeller speed,

$$\frac{\partial \dfrac{Q_p}{N_{p(max)}\, I_p \left[1 + \dfrac{I_e}{I_p/R^2}\right]}}{\partial \dfrac{N_p}{N_{p(max)}}}, \frac{1}{\text{sec}}$$

f_1 function of W_f, N_e

f_2 function of β, N_p

i imaginary number, $\sqrt{-1}$

I_e polar moment of inertia of rotating parts of engine, (lb)(ft)(sec)(rad)(min)/revolution

I_p polar moment of inertia of propeller, (lb)(ft)(sec)(rad)(min)/revolution

K arbitrary constant

K_1 constant defining equilibrium condition, $K_1 = \frac{a_1}{b_1 + d_1}$, $\frac{\text{rpm}}{\text{lb/hr}}$

K_2 constant defining equilibrium condition, $K_2 = \frac{c_1}{b_1 + d_1}$, $\frac{\text{rpm}}{\text{deg}}$

N_e engine speed, rpm

N_p propeller speed, rpm

Q_e engine torque, lb-ft

Q_p propeller torque, lb-ft

R gear ratio of engine speed to propeller speed

W_f fuel flow, lb/hr

β propeller-blade angle, deg

β_a beta arm, used to denote lever input to mechanism for changing propeller-blade angle on engine used to run data

Δ deviation from initial operating point

τ engine time constant, sec

ω frequency, radians/sec

Subscript:

max maximum

REFERENCES

1. Brown, Gordon S., and Campbell, Donald P.: Principles of Servomechanisms. John Wiley & Sons, Inc., 1948.

2. Otto, Edward W., and Taylor, Burt L., III: Dynamics of a Turbojet Engine Considered as a Quasi-Static System. NACA TN 2091, 1950.

TABLE I - STEADY-STATE AND TRANSIENT CHARACTERISTICS OF INSTRUMENTS

Measured variable	Steady-state accuracy	Transient characteristics
Blade angle, β	$\frac{1}{2}^{\circ}$	Limited by oscillograph element (40 cps)
Beta arm, β_a	1 percent of full travel	Limited by oscillograph element (40 cps)
Fuel flow, W_f	±1 percent for full flow	10-15 cps
Torque, Q	±1 percent for full scale	- - - - - - - - - - - - - -
Engine speed, N_e	$\frac{1}{3}$ of 1 percent for full scale	Limited by filter circuit (1.59 cps)

TABLE II - FREQUENCY-RESPONSE FUNCTIONS

1	2	3	4
Frequency-response function	Operating point	Algebraic form of frequency-response function from experimental data	Algebraic form of frequency-response function from calculated equation
$\frac{\Delta N_e/N_{e(max)}}{\Delta\beta}(i\omega)$ (percent/deg)	General	$\frac{K}{(1+i\tau_1\omega)(1+i\tau_2\omega)}$	$\frac{K_2}{(1+i\tau\omega)}$
	W_f=65 percent of maximum rated	$\frac{-1.06}{(1+i3.05\omega)(1+i0.283\omega)}$	$\frac{-1.06}{(1+i3.75\omega)}$
	W_f=81 percent of maximum rated	$\frac{-1.73}{(1+i3.35\omega)(1+i0.185\omega)}$	$\frac{-1.76}{(1+i2.86\omega)}$
$\frac{\Delta N_e/N_{e(max)}}{\Delta W_f/W_{f(max)}}(i\omega)$ (percent)	General	$\frac{K}{(1+i\tau_1\omega)(1+i\tau_2\omega)}$	$\frac{K_1}{(1+i\tau\omega)}$
	β =18°	$\frac{76}{(1+i3.32\omega)(1+i0.375\omega)}$	$\frac{75}{(1+i3.75\omega)}$
	β =28°	$\frac{50}{(1+i2.73\omega)(1+i0.332\omega)}$	$\frac{48}{(1+i2.86\omega)}$

NACA

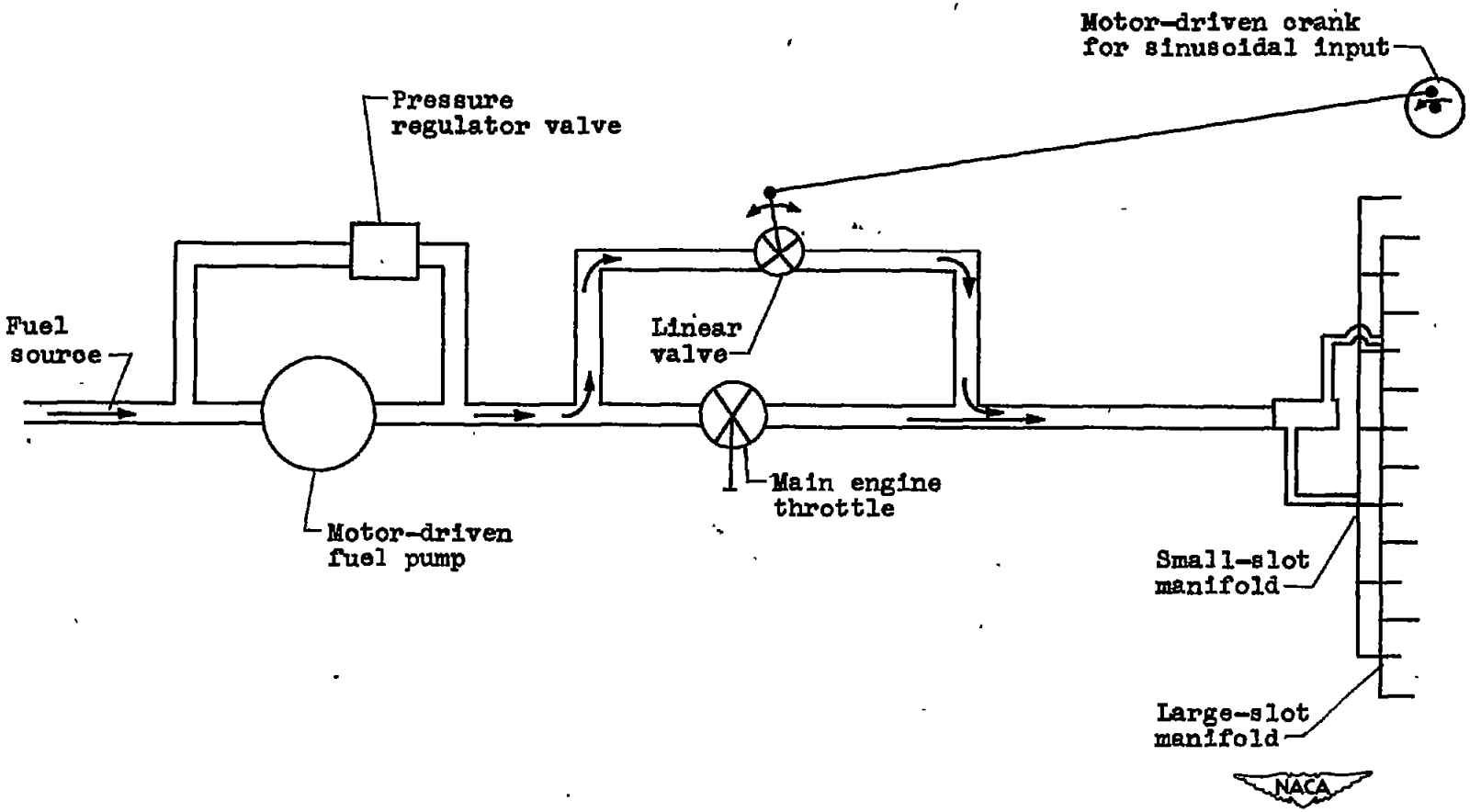

Figure 1. - System for providing sinusoidal fuel flow.

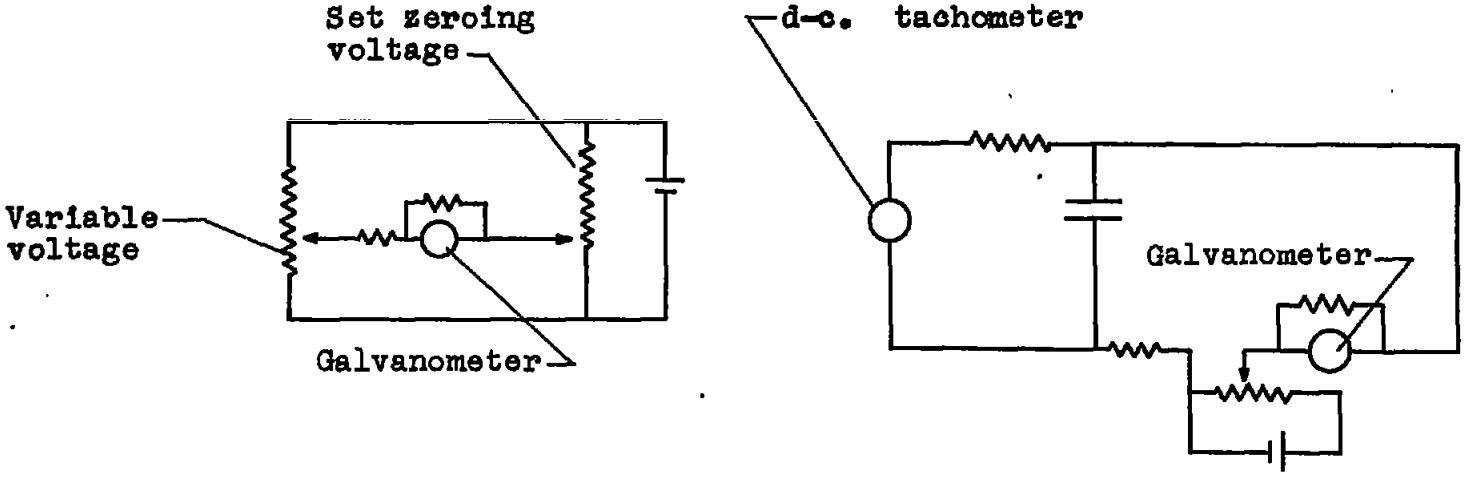

(a) Typical circuit for measurement of position.

(b) Circuit for transient-speed measurement.

Figure 2. - Schematic diagrams of transient response instrumentation.

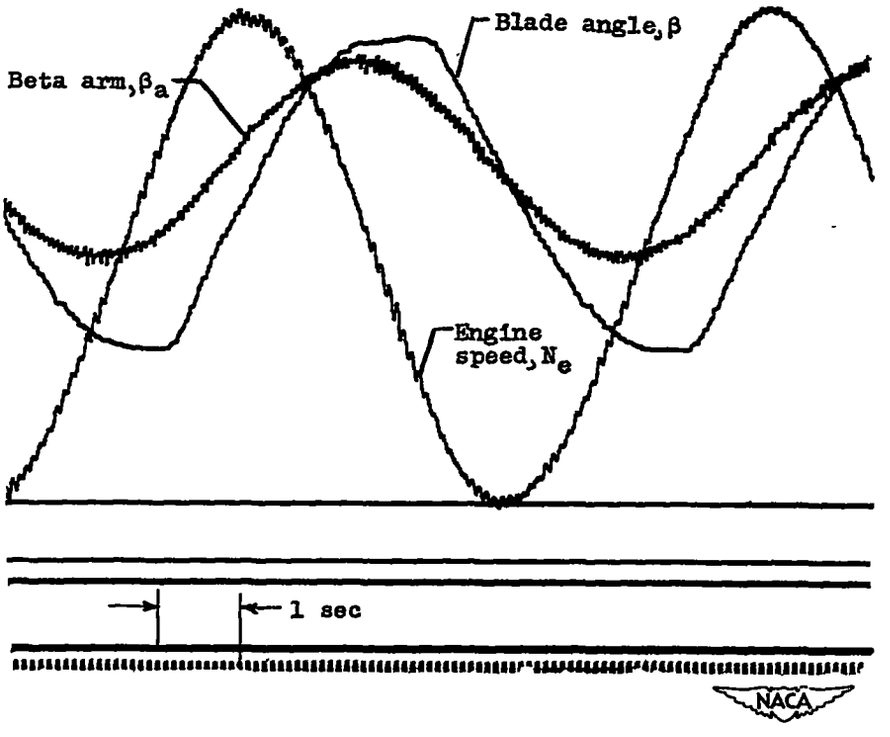

(a) Typical data showing steady-state sinusoidal response of engine speed to blade angle. Fuel flow, 81 percent of maximum rated; mean engine speed, 92.5 percent of maximum; mean blade angle, 28°; frequency, 0.986 radian per second.

Figure 3. - Typical steady-state sinusoidal data for turbine-propeller engine.

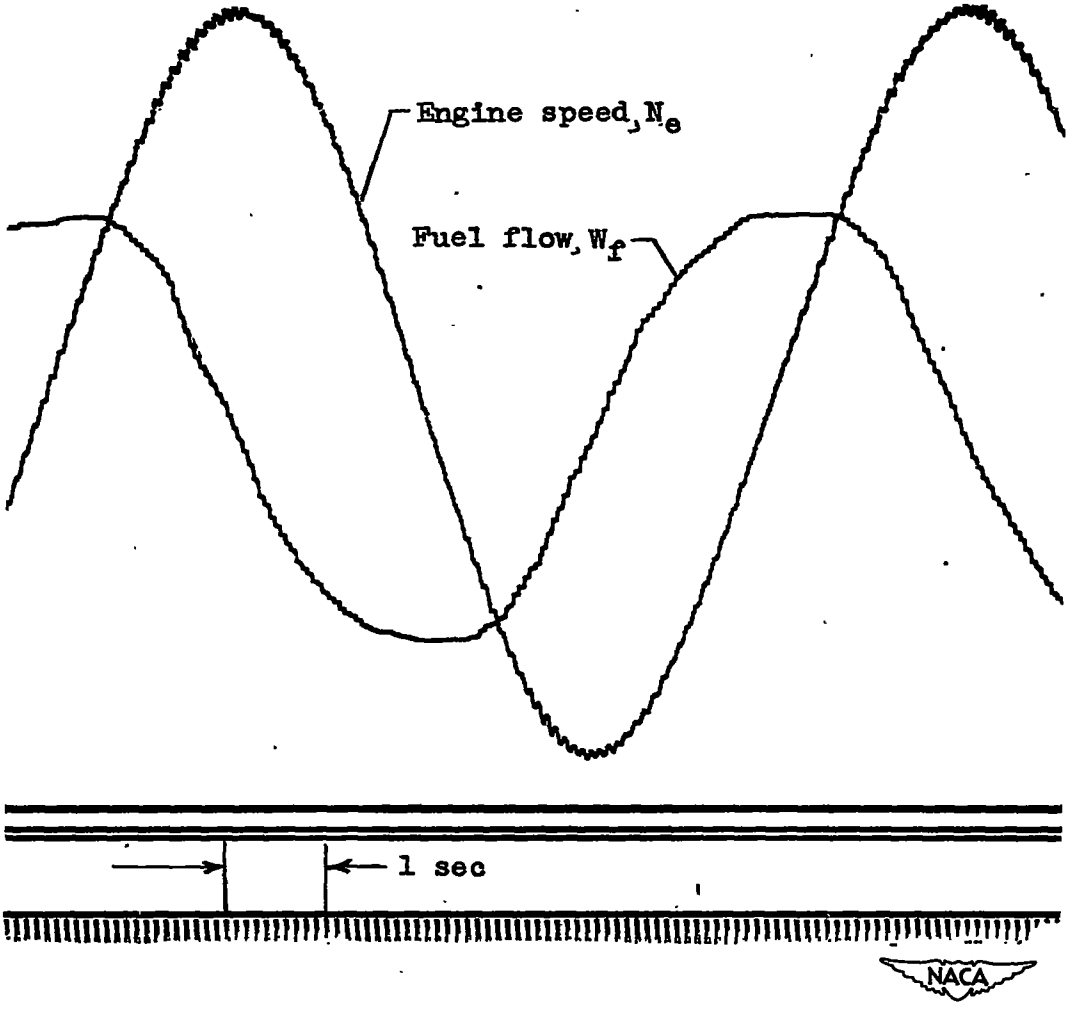

(b) Typical data showing steady-state sinusoidal response of engine speed to fuel flow. Blade angle, 18°; mean engine speed, 97.5 percent of maximum; mean fuel flow, 65 percent of maximum rated; frequency, 0.873 radian per second.

Figure 3. - Concluded. Typical steady-state sinusoidal data for turbine-propeller engine.

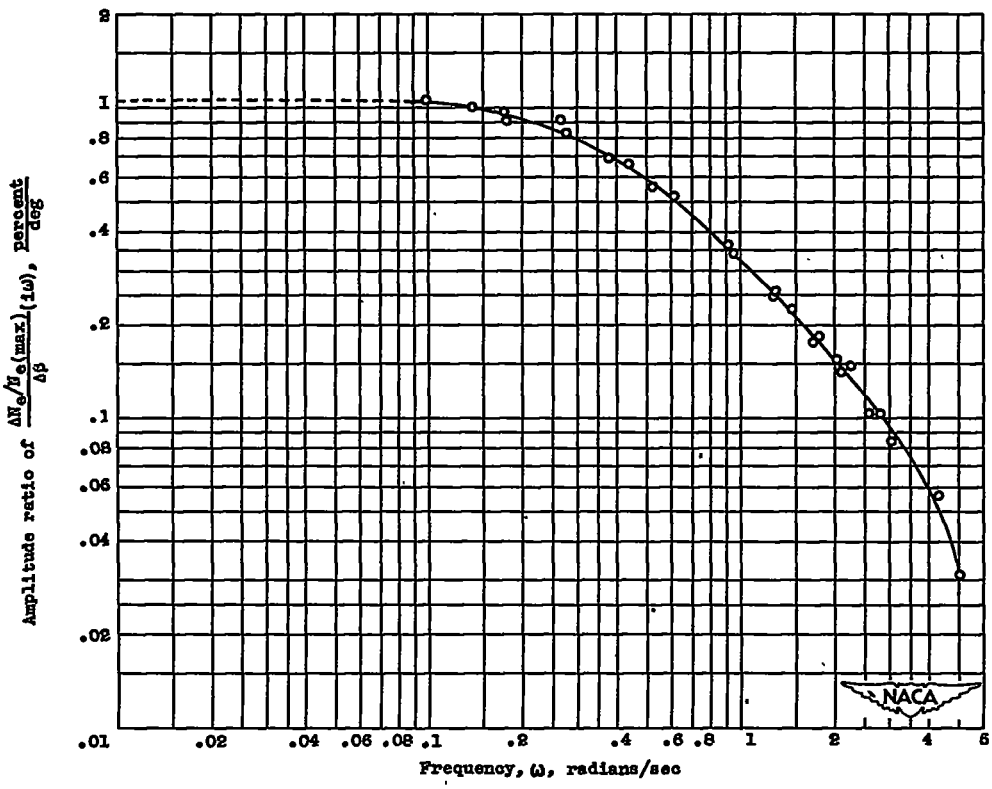

(a) Amplitude-ratio relation. Fuel flow, 65 percent of maximum rated; mean engine speed, 97.6 percent of maximum; mean blade angle, 18°; blade-angle amplitude, 2°.

Figure 4. - Propeller-blade angle - engine-speed relations at constant fuel flow obtained from experimental sinusoidal response data for typical turbine-propeller engine.

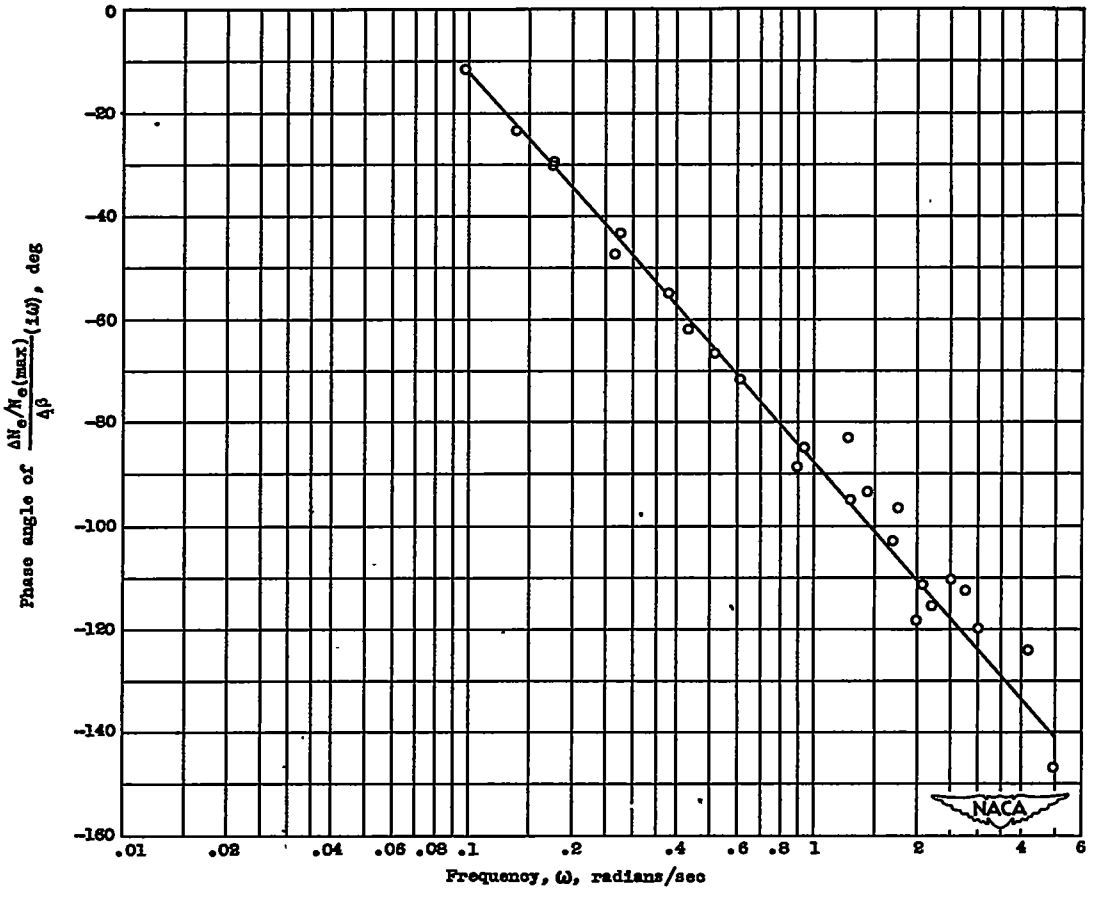

(b) Phase-angle relation. Fuel flow, 65 percent of maximum rated; mean engine speed, 97.5 percent of maximum; mean blade angle, 18°; blade-angle amplitude, 2°.

Figure 4. - Continued. Propeller-blade angle - engine-speed relations at constant fuel flow obtained from experimental sinusoidal response data for typical turbine-propeller engine.

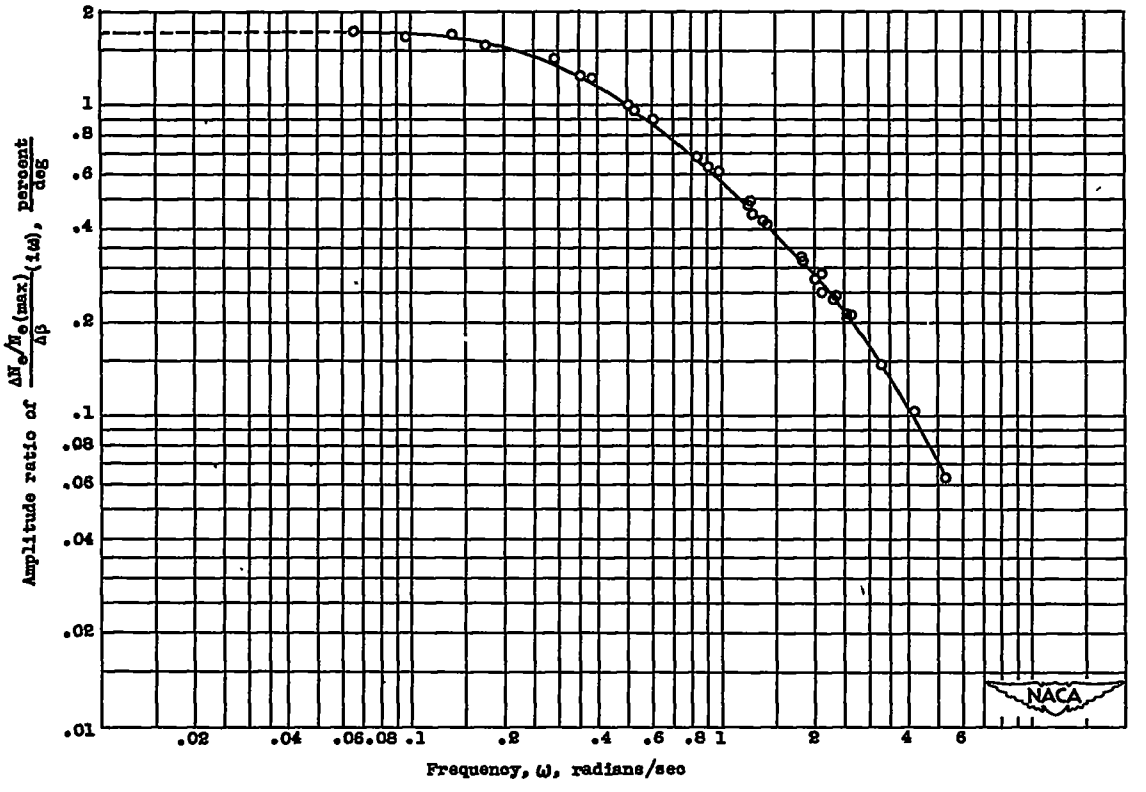

(c) Amplitude-ratio relation. Fuel flow, 81 percent of maximum rated; mean engine speed, 92.5 percent of maximum; mean blade angle, 28°; blade-angle amplitude, 2°.

Figure 4. - Continued. Propeller-blade angle - engine-speed relations at constant fuel flow obtained from experimental sinusoidal response data for typical turbine-propeller engine.

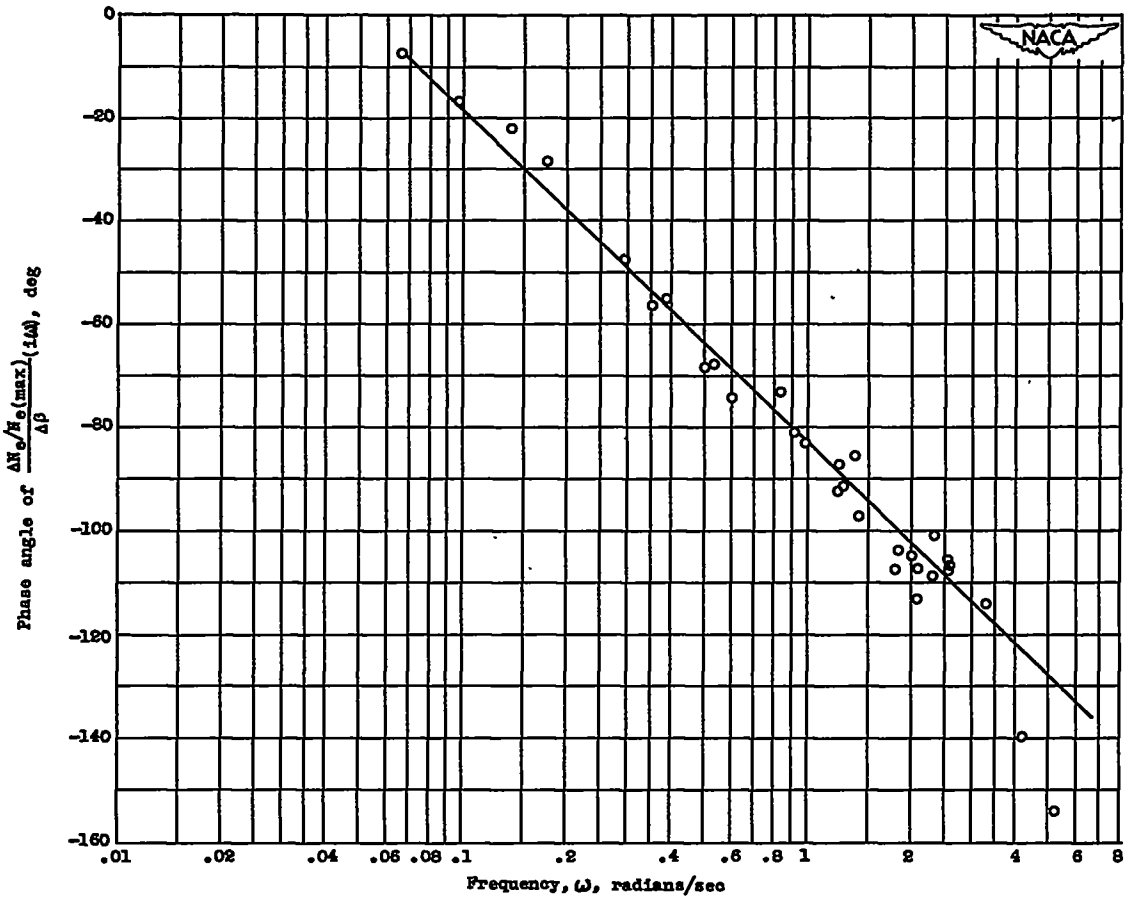

(d) Phase-angle relation. Fuel flow, 81 percent of maximum rated; mean engine speed, 92.5 percent of maximum; mean blade angle, 28°; blade-angle amplitude, 2°.

Figure 4. - Concluded. Propeller-blade angle - engine-speed relations at constant fuel flow obtained from experimental sinusoidal response data for typical turbine-propeller engine.

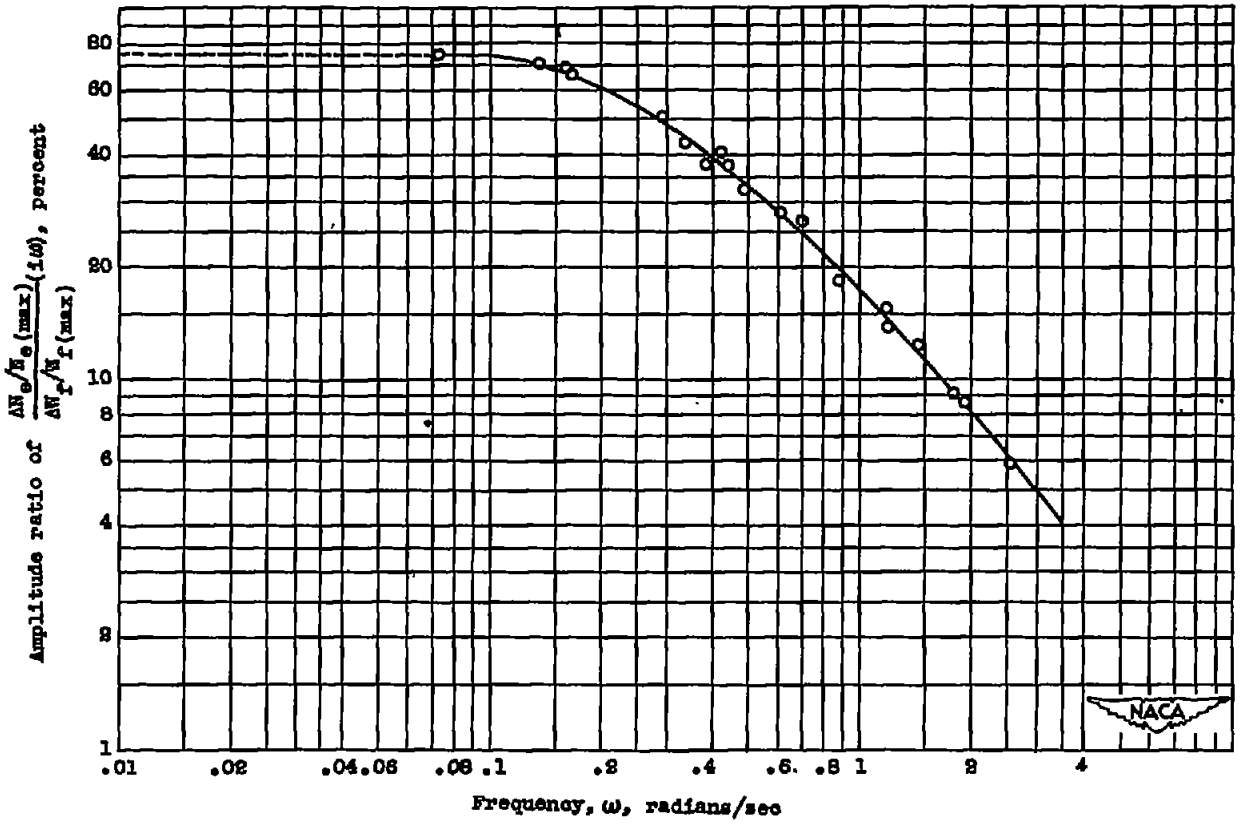

(a) Amplitude-ratio relation. Mean fuel flow, 65 percent of maximum rated; mean engine speed, 97.5 percent of maximum; blade angle, 18°; fuel-flow amplitude, 3.9 percent of maximum.

Figure 5. - Fuel-flow - engine-speed relations at constant blade angle obtained from experimental sinusoidal response data for typical turbine-propeller engine.

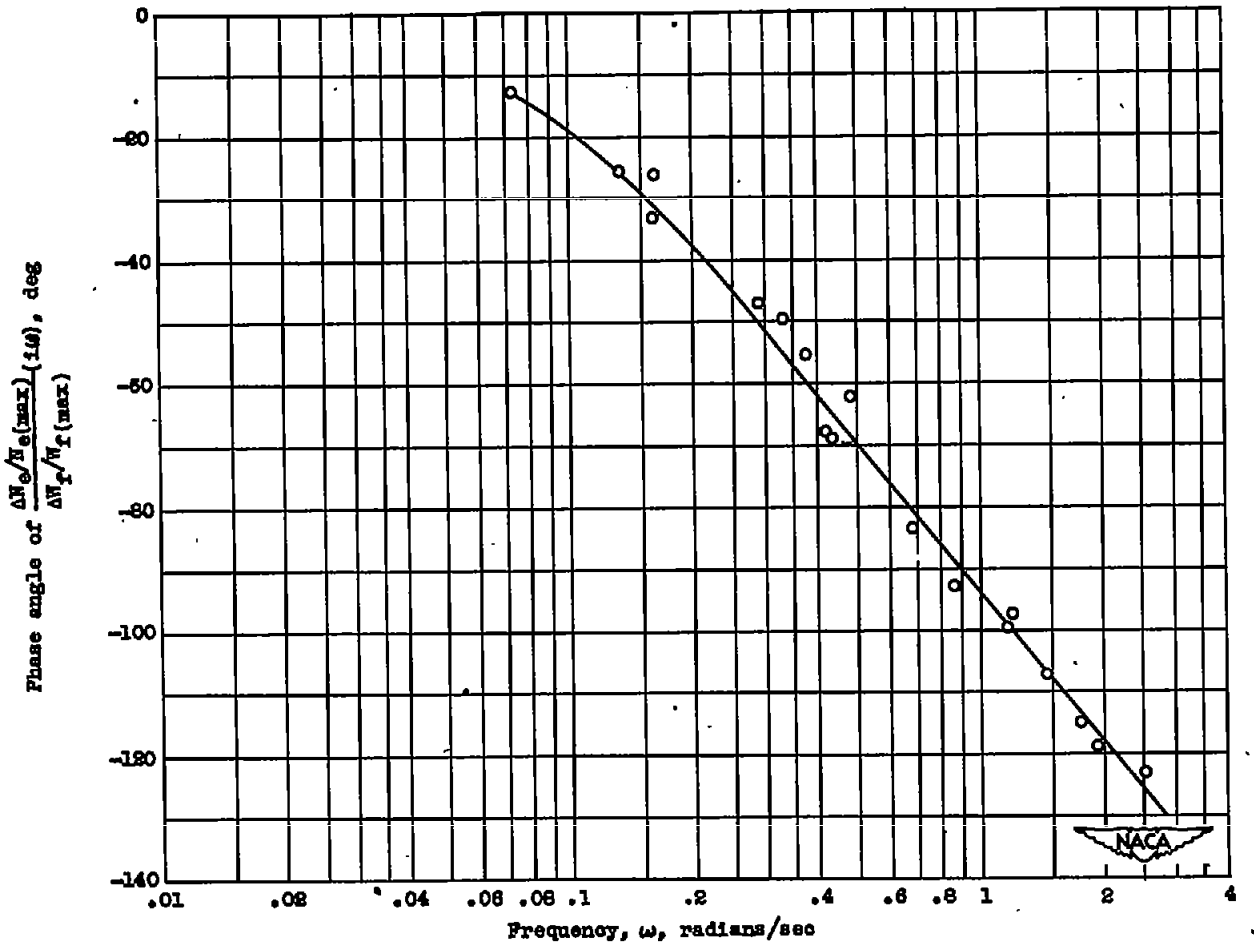

(b) Phase-angle relation. Mean fuel flow, 65 percent of maximum rated; mean engine speed, 97.5 percent of maximum; blade angle, 18°; fuel-flow amplitude, 5.9 percent of maximum.

Figure 5. - Continued. Fuel-flow - engine-speed relations at constant blade angle obtained from experimental sinusoidal response data for typical turbine-propeller engine.

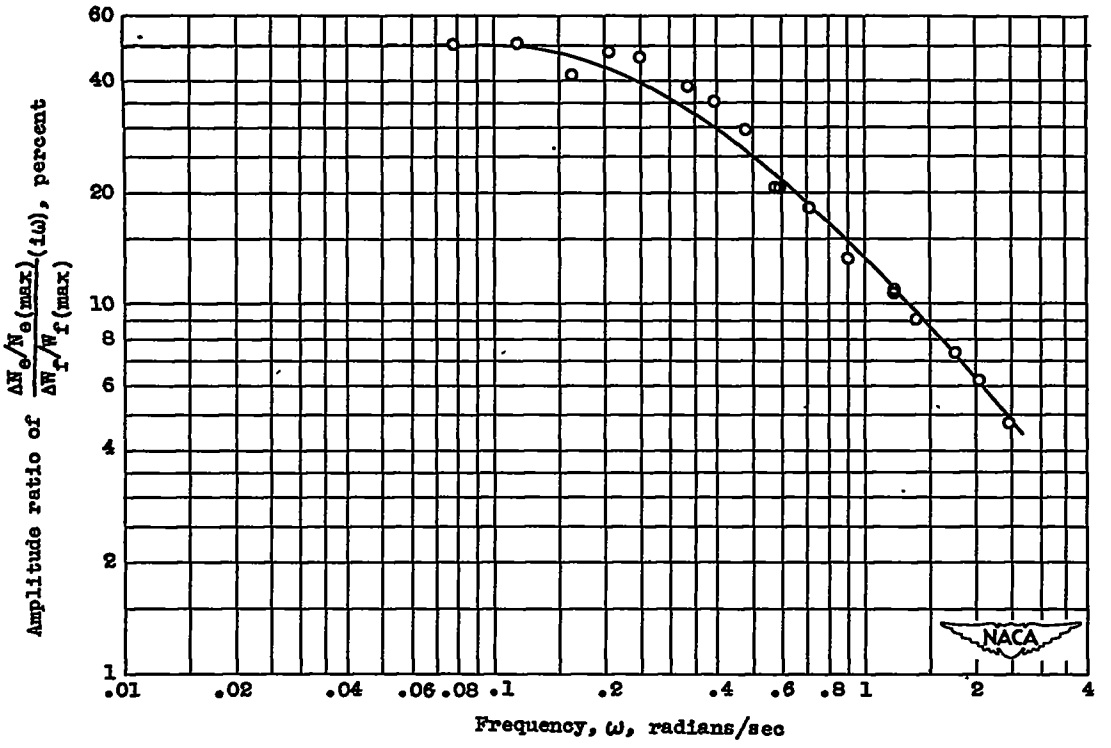

(c) Amplitude-ratio relation. Mean fuel flow, 81 percent of maximum rated; mean engine speed, 92.5 percent of maximum; blade angle, 28°; fuel-flow amplitude, 3.9 percent of maximum.

Figure 5. - Continued. Fuel-flow - engine-speed relations at constant blade angle obtained from experimental sinusoidal response data for typical turbine-propeller engine.

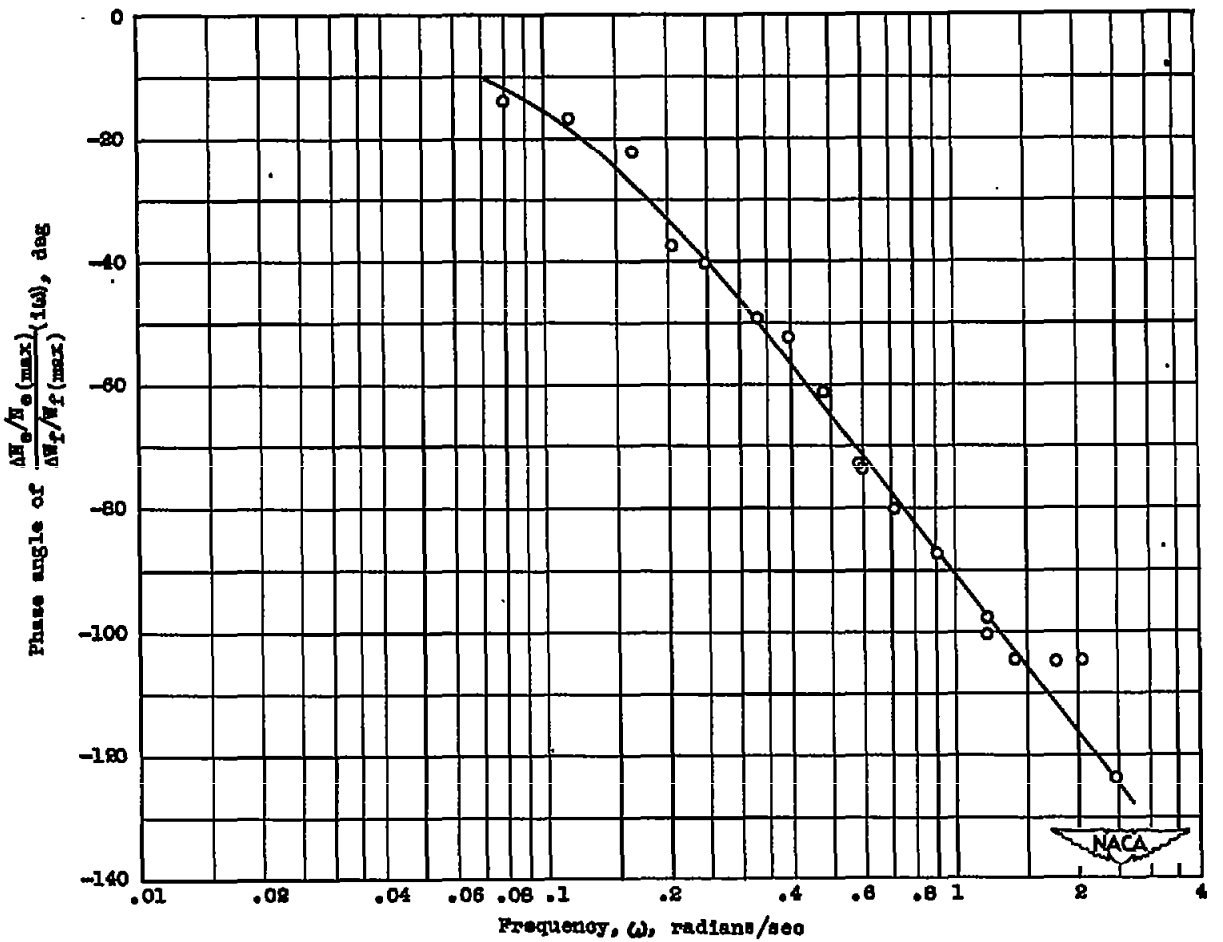

(d) Phase-angle relation. Mean fuel flow, 81 percent of maximum rated; mean engine speed, 98.6 percent of maximum; blade angle, 28°; fuel-flow amplitude, 3.9 percent of maximum.

Figure 5. - Concluded. Fuel-flow - engine-speed relations at constant blade angle obtained from experimental sinusoidal response data for typical turbine-propeller engine.

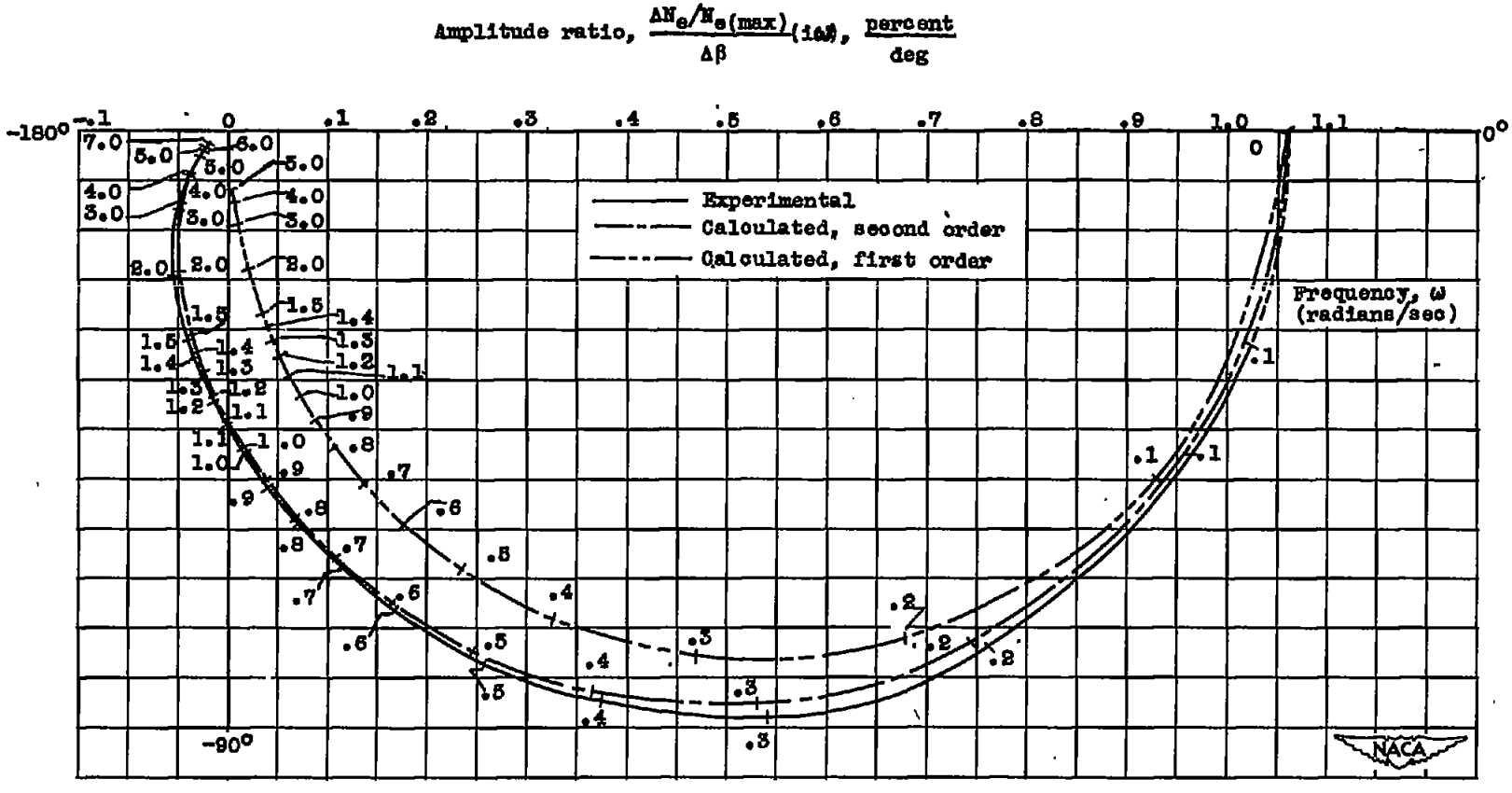

(a) Fuel flow, 65 percent of maximum rated; mean engine speed, 97.5 percent of maximum; mean blade angle, 18°.

Figure 6. - Frequency response of engine speed to variations in propeller-blade angle obtained from experimental data and theoretical calculations for typical turbine-propeller engine.

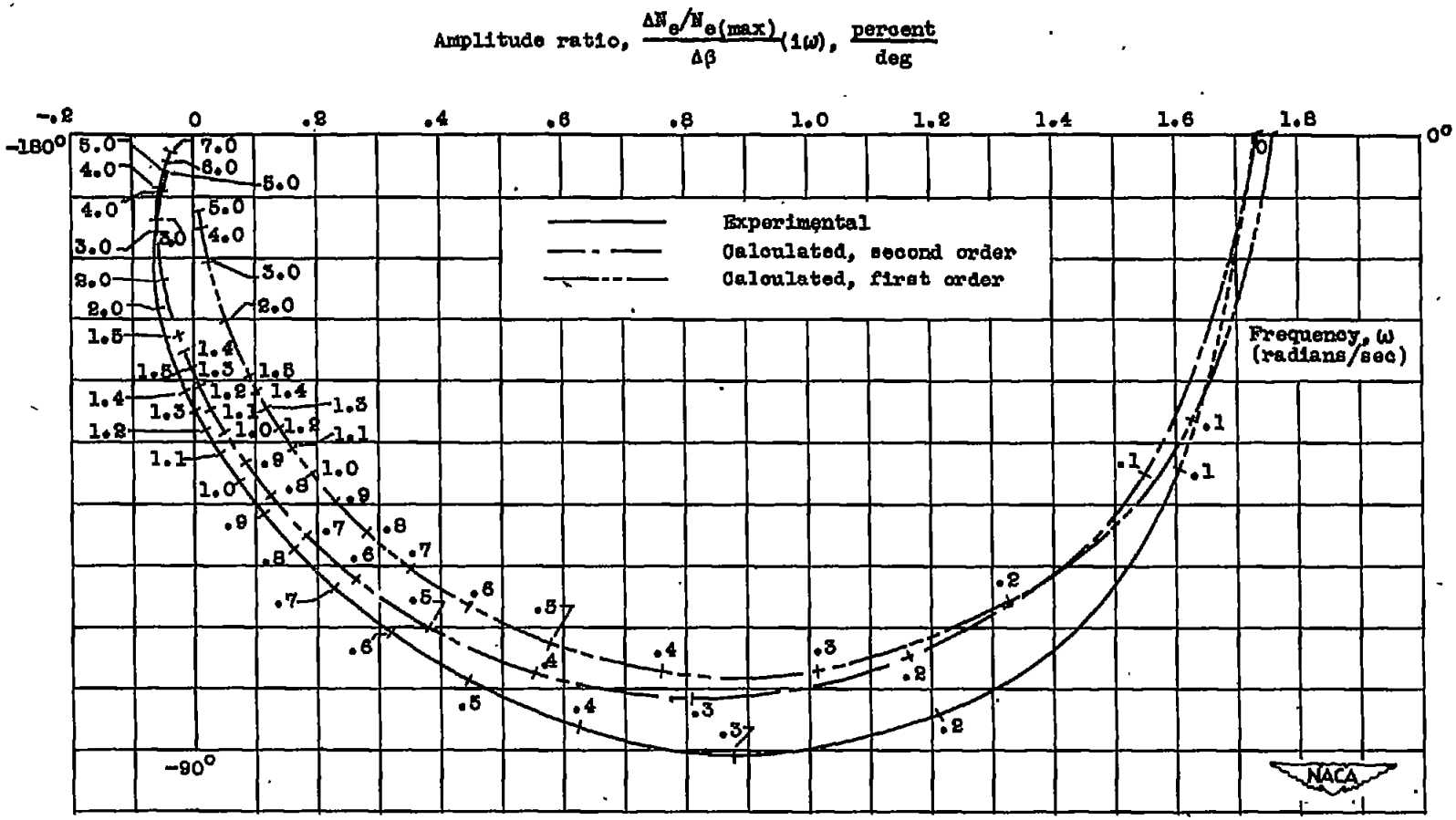

(b) Fuel flow, 81 percent of maximum rated; mean engine speed, 92.5 percent of maximum; mean blade angle, 28°.

Figure 6. - Concluded. Frequency response of engine speed to variations in propeller-blade angle obtained from experimental data and theoretical calculations for typical turbine-propeller engine.

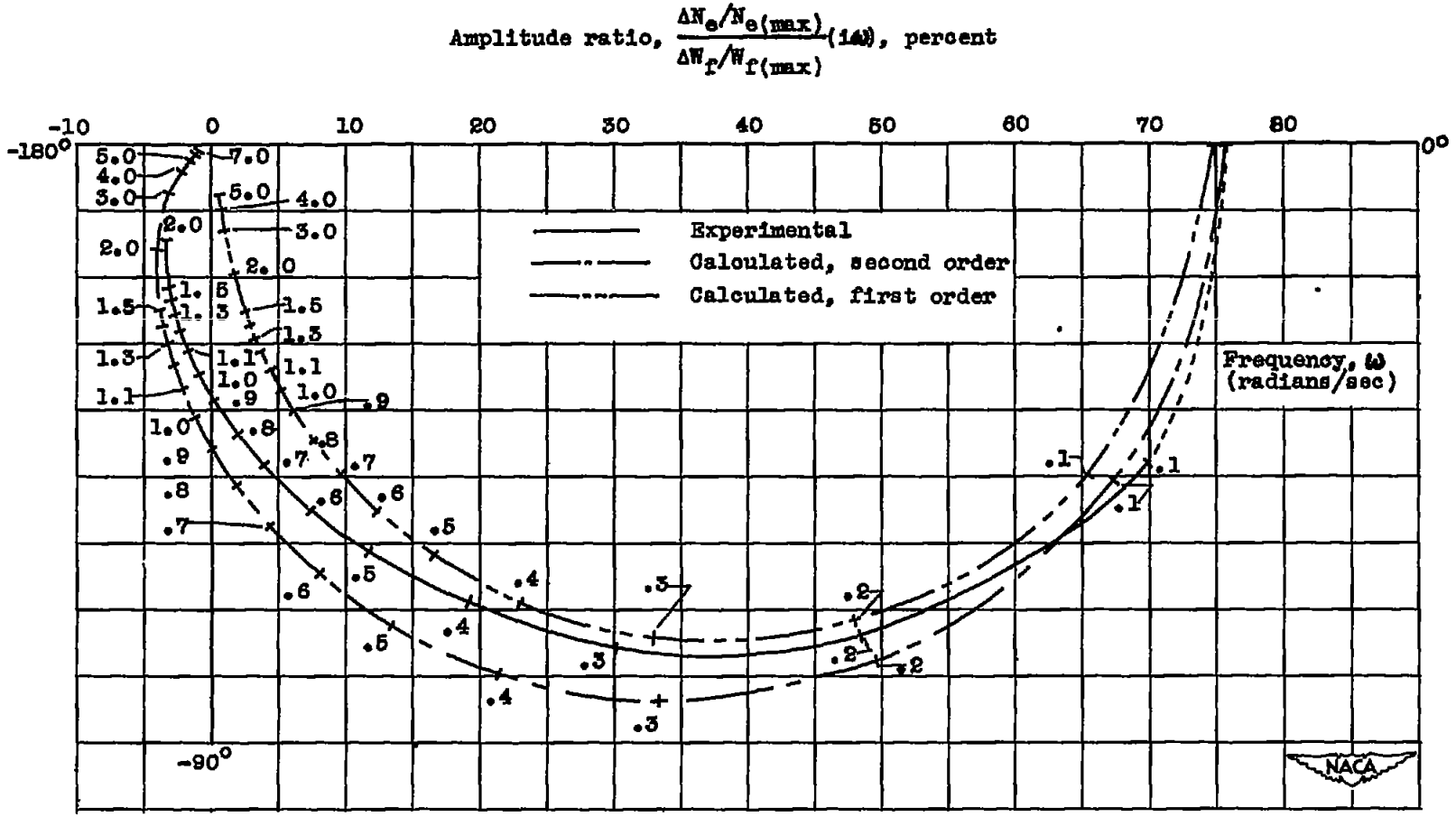

(a) Mean fuel flow, 65 percent of maximum rated; mean engine speed, 97.5 percent of maximum; blade angle, 18°.

Figure 7. - Frequency response of engine speed to variations in fuel flow obtained from experimental data and theoretical calculations for typical turbine-propeller engine.

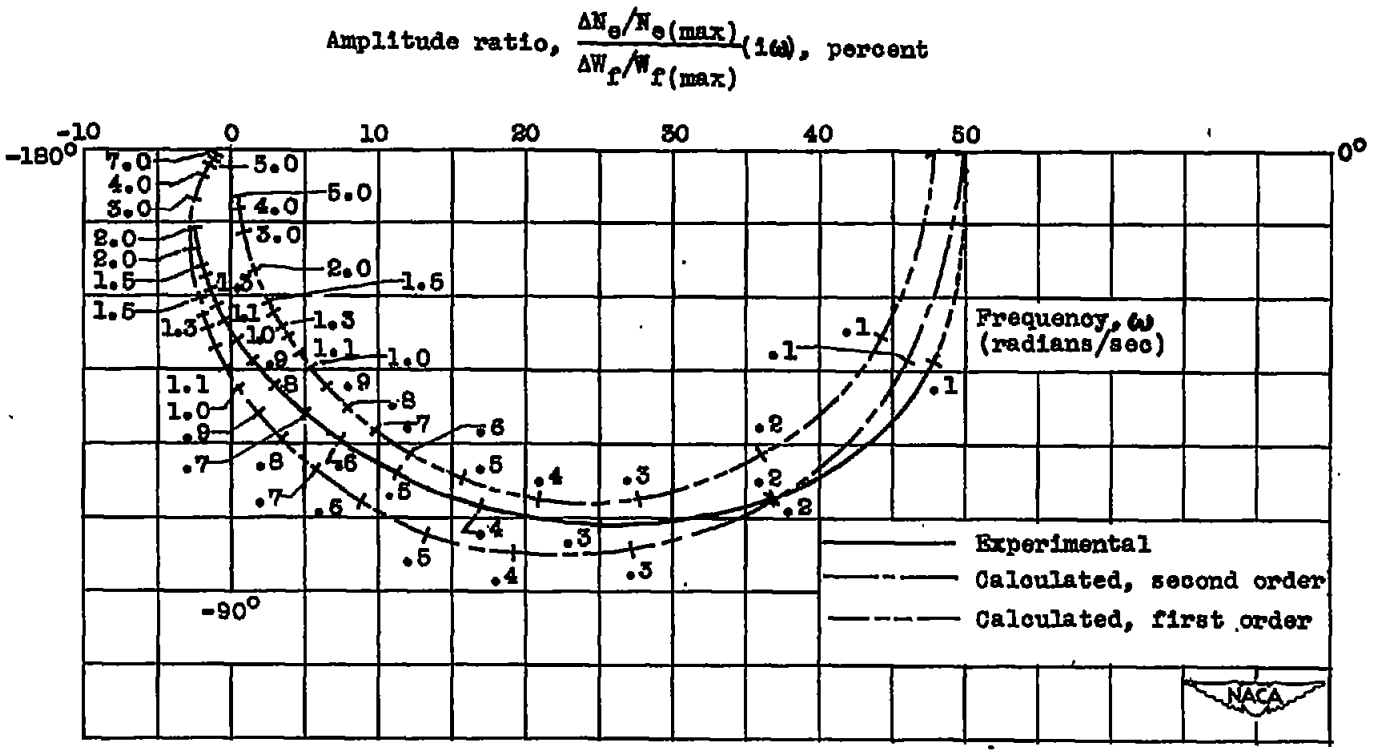

(b) Mean fuel flow, 81 percent of maximum rated; mean engine speed, 92.5 percent of maximum; blade angle, 28°.

Figure 7. - Concluded. Frequency response of engine speed to variations in fuel flow obtained from experimental data and theoretical calculations for typical turbine-propeller engine.

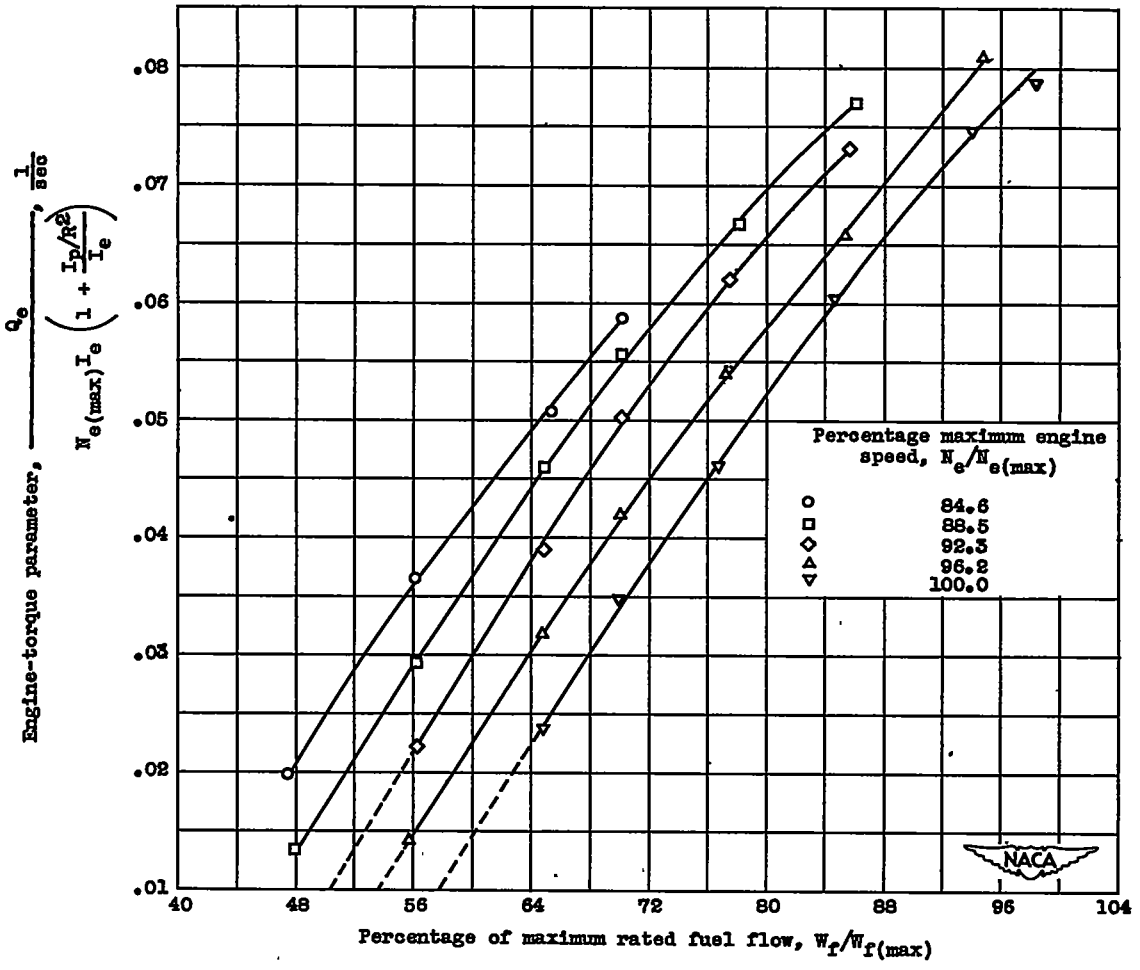

(a) Constant engine-speed characteristics.

Figure 8. - Relation between engine-torque parameter, percentage of maximum engine speed, and percentage of maximum rated fuel flow as obtained from experimental data for typical turbine-propeller engine.

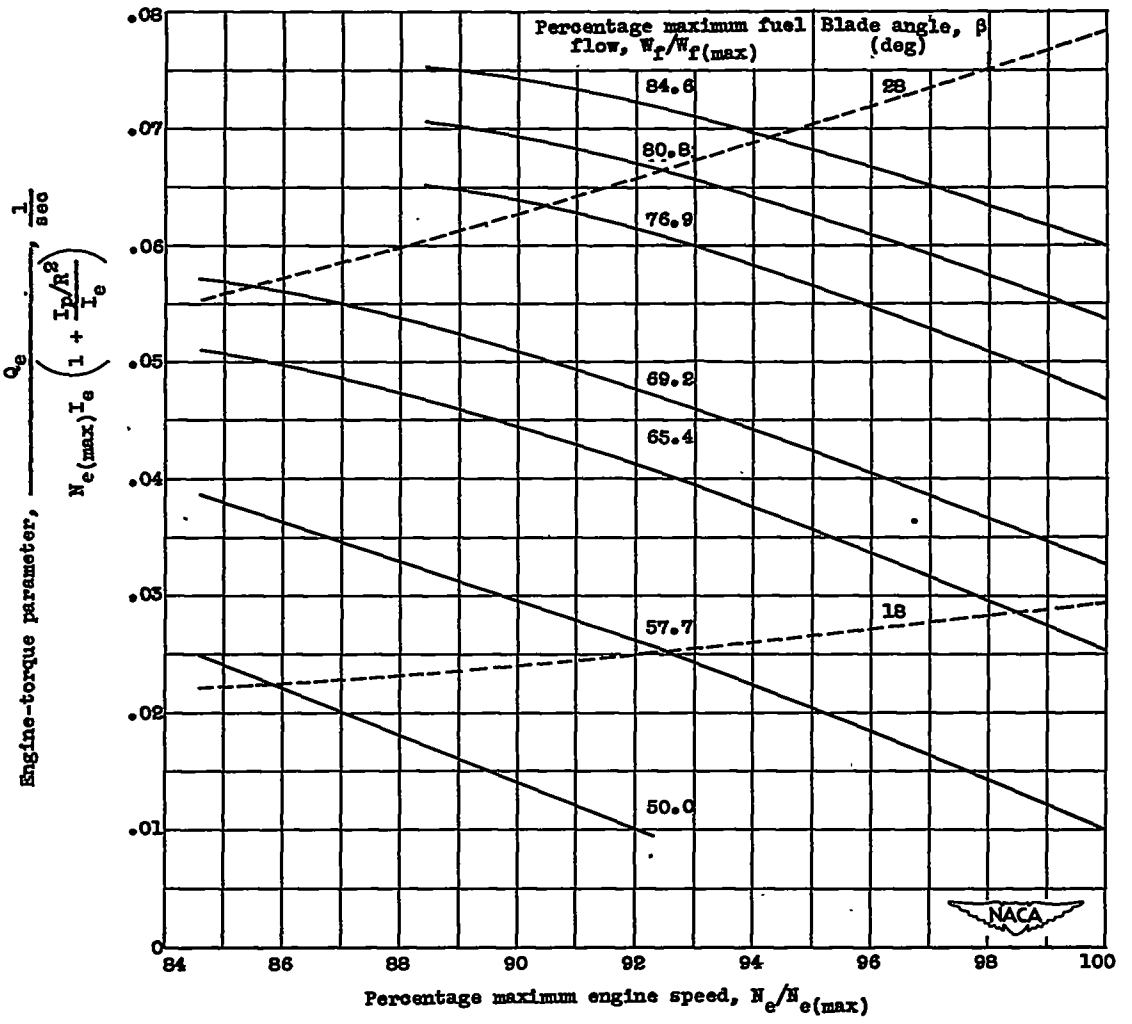

(b) Constant fuel-flow characteristics including selected operating lines.

Figure 8. - Concluded. Relation between engine-torque parameter, percentage of maximum engine speed, and percentage maximum rated fuel flow as obtained from experimental data for typical turbine-propeller engine. (Cross-plotted from fig. 8(a).)

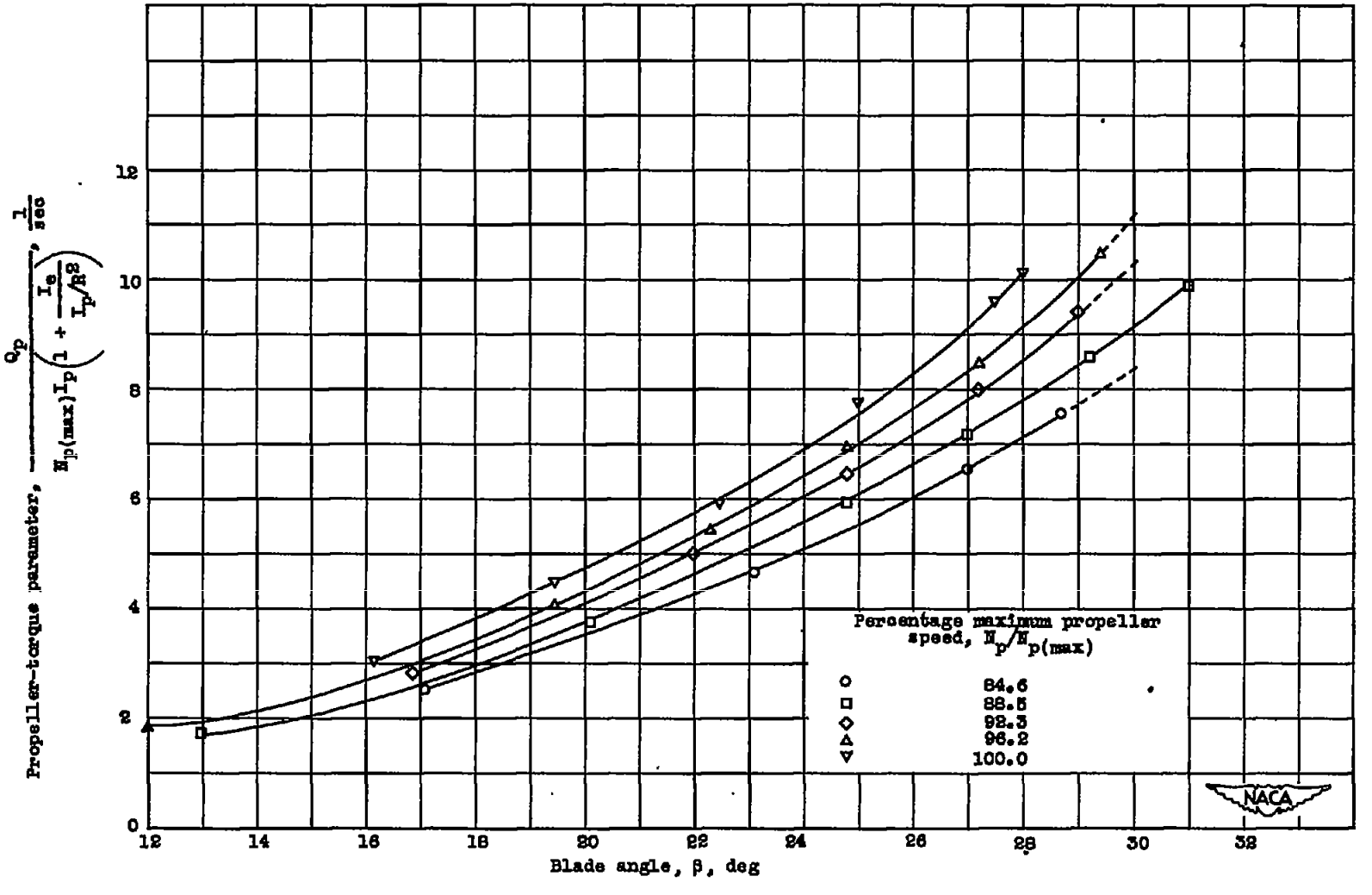

(a) Constant propeller-speed characteristics.

Figure 9. - Relations between propeller-torque parameter, percentage maximum propeller speed, and blade angle for 12-foot-1-inch-diameter, four-bladed propeller.

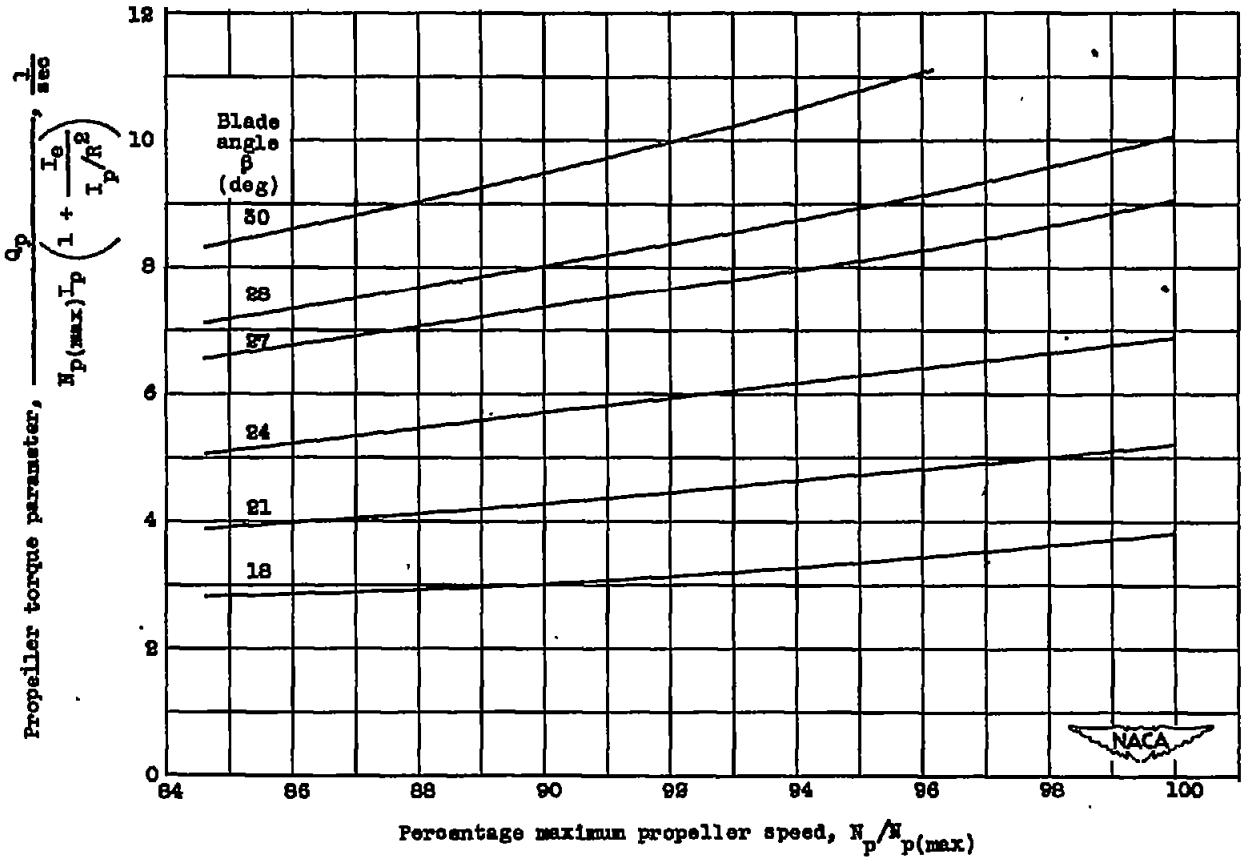

(b) Constant blade-angle characteristics. (Cross-plotted from fig. 9(a).)

Figure 9. - Concluded. Relations between propeller torque parameter, percentage maximum propeller speed, and blade angle for 12-foot-1-inch-diameter, four-bladed propeller.